ISTITUTO NAZIONALE DI FISICA NUCLEARE

Sezione di Milano

INFN/TC–99/08
9 Aprile 1999

DEVELOPMENT OF AN X–RAY SPECTROMETER FOR HIGH LATERAL RESOLUTION XRF ANALYSIS

L. Bonizzoni[1], C. Cicardi[2,3], C. De Martinis[2,3], A. Galli[1], M. Milazzo[1]

[1]Università degli Studi di Milano, Istituto di Fisica Generale Applicata (IFGA), Via Celoria 16, I–20133 Milano, Italy
[2]INFN–Sezione di Milano, Via Celoria 16, I–20133 Milano, Italy
[3]Università degli Studi di Milano, Dipartimento di Fisica, Via Celoria 16, I–20133 Milano, Italy

Abstract

A table–top micro beam XRF spectrometer based on the properties of capillary optics has been realised.

The system is equipped with two beam lines obtained by microcapillary collimators with inner diameter of 400 μm and 100 μm respectively.

The X–ray probe has been characterised in terms of spectral monocromaticity, intensity gain, lateral resolution, beam divergence and intensity.

Preliminary applications on ancient layered glasses and plaster detachment stratigraphies are presented.

The advantage of the coupling of the microcapillary collimators with an already installed PIXE induced – XRF source is also discussed.

PACS.: 07.85

*Published by **SIS–Pubblicazioni***
Laboratori Nazionali di Frascati

1. – INTRODUCTION

The use of an X–ray beam in micro–fluorescence analysis has several advantages over the typical use of an electron microprobe. These advantages include the ability to operate in air, the possibility of performing non destructive analysis, high peak to background ratio and the possibility to avoid interelemental effects. On the other hand, the primary disadvantage of an X–ray beam is the lower intensity.

Typically, X–ray micro–fluorescence instruments make use of pinhole diaphragms to restrict the size of the beams emerging from X–ray tubes (fine focus or micro focus). This arrangement is limited because of the low intensity and the non–uniform profile of the beam from a metal aperture[1, 2].

Previous works[3, 4, 5] have shown that the use of capillary optics increases the transmitted intensity from a laboratory X–ray source up to about 5 x 10^2 times. Due to the total reflection of X–rays on the inner walls of a glass pipe, a large solid angle $\Delta\omega_{eff}$ of the emitted radiation is transported to the target (Fig. 1). Several authors[6] have shown that a uniform X–ray beam is obtained with a sufficient intensity to permit accurate high lateral resolution micro–XRF analysis.

In the present work, we show also the foreseen advantage arising from the use of capillary wave guides coupled with a PIXE induced–XRF source. In fact, as shown in ref. (7), exploiting the high intensity at low energies of the PI–XRF technique and the dependence of the capillary gain factor from energy, we plan to develop an intense monochromatic X–ray source, in the energy range 4 to 10 keV, with a size spot of 100 or 400 μm. The availability of this kind of X–ray source should be very useful for applications in the field of cultural and environmental diagnostics.

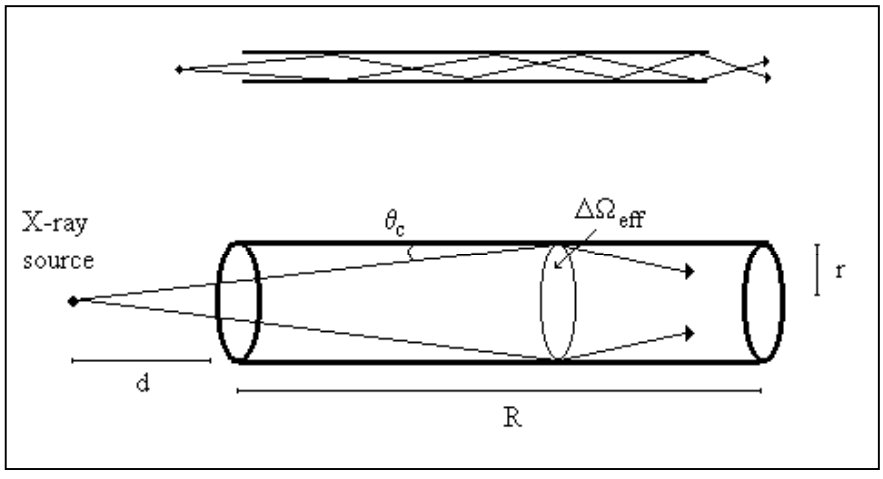

FIG. 1 – Schematic diagram of the beam path inside the capillary from a point source. Note that the "effective" solid angle $\Delta\Omega_{eff} = \pi \sin^2(\theta_c)$ is related to the critical angle for total reflection θ_c.

2. – EXPERIMENTAL SET–UP

X–ray tubes: Conventional AEG long fine – and micro – focus diffraction X–ray tubes have been used, with Cu and Mo anodes. The maximum power loading was 800 W for the Cu tube and 2000 W for the Mo one.

For both fine – and micro – focus tubes, focal point output was used at a small take off angle (about 5°) geometry to achieve high virtual brilliance which can be efficiently utilised by the capillary wave–guide.

Tube–capillary coupling: In order to increase the stability of the system and to permit a good alignment of the capillary optics with the X–ray beam emerging from the anode, an aluminium support was rigidly fasten to the tube shielding as shown in Fig. 2.

The capillary was encapsulated and fixed in a brass holder filled with a semi–solid silicon–paste containing tungsten to prevent radiation leakage. The holder was fitted into a standard 5 axis gimbals (Newport LP–05B) and put in close proximity to the Be windows corresponding to the focal output on the X–ray tube shielding. The gimbals allowed for a precise positioning in the plane perpendicular to the beam. Vertical and horizontal tilt angles were also adjustable, in order to achieve maximum transmitted intensity.

Beam alignment: In order to localise the beam spot position on the target, we used a fluorescent screen. A microscope points at the spot as shown in Fig. 3 and a grating lens defines the area to be analysed, after the removing of the fluorescent screen.

Detector – sample alignment: To increase the detection efficiency, a laser pointer mounted on the top of the detector produces, by a movable mirror, a beam coaxial with the axis of the active volume, which lights the area of interest.

The spectrometer: The whole system, composed of X–ray tube, microscope, capillaries and Si(Li) detector, is shown in Fig. 4.

To perform XRF analysis of objects of different dimensions, the X–ray tube was positioned vertically. In this way we could also use both tube Be windows corresponding to the point focal output, so achieving two different beam lines.

The capillary inner diameter and the length were chosen 100 μm, 200 mm and 400 μm, 200 mm, respectively, well suited for our purpose.

The detector was mounted on a movable plane to permit the alternate use of the two beam lines.

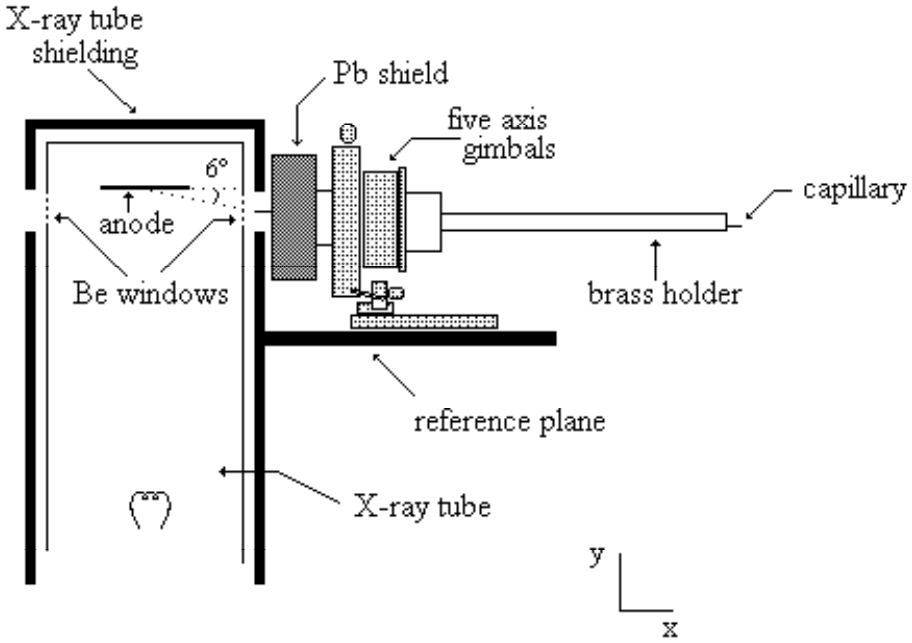

FIG. 2 – Sketch of capillary–tube coupling.

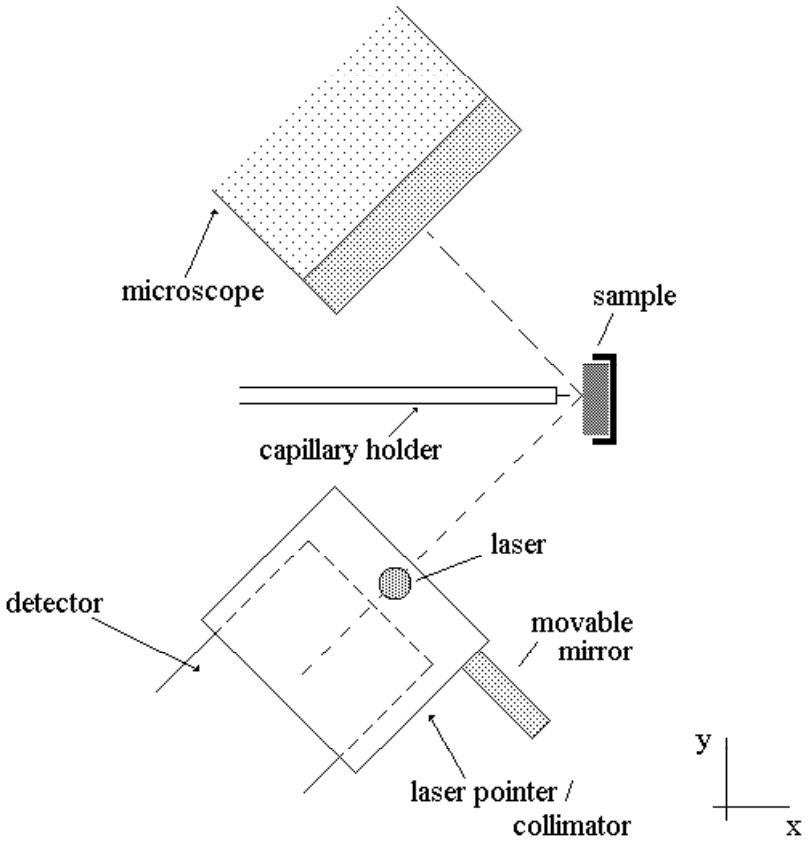

FIG. 3 – Relative position of capillary, sample, detector and microscope.

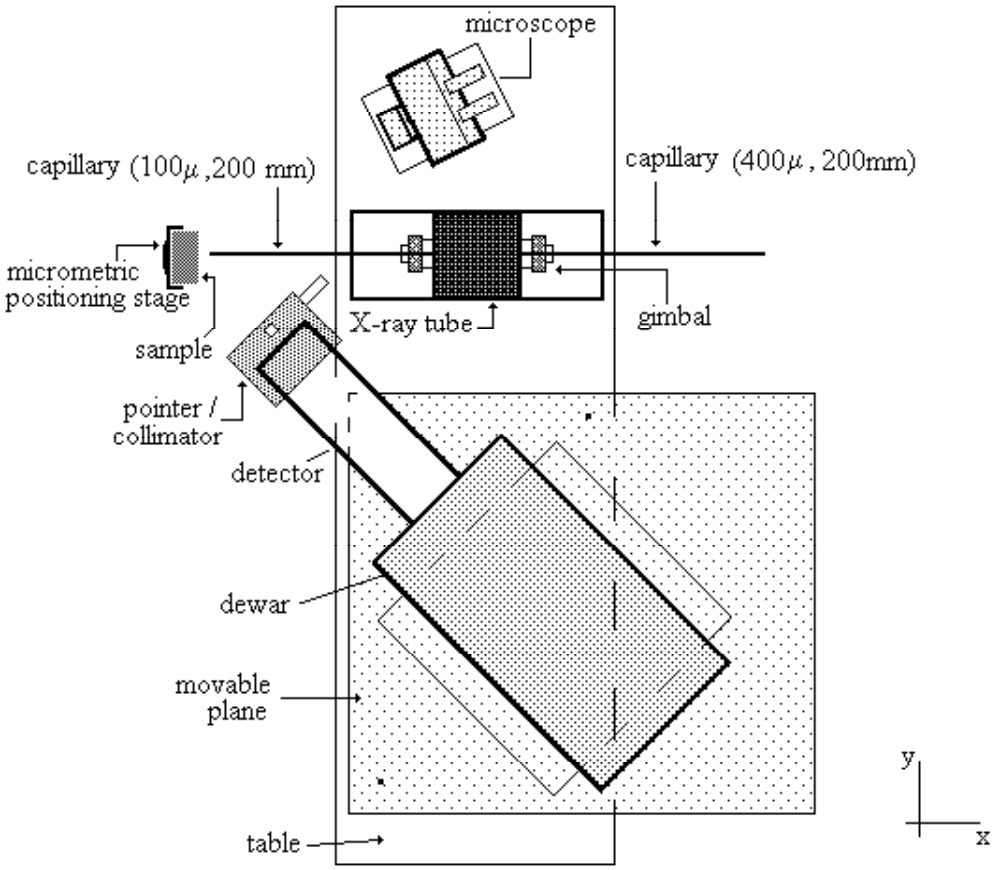

FIG. 4 – Schematic representation (not in scale) of the whole system.

3. – MEASUREMENTS AND RESULTS

Gain factor: The gain factor is defined as the ratio between the intensity transmitted by a capillary wave–guide and that emerging from a pinhole diaphragm, in the same geometrical conditions. This factor can be written, for an ideal cylindrical capillary, as[3] :

$$G = \sin^2\theta_c \left(\frac{d + R}{r}\right)^2$$

where R is the capillary length, r the inner radius, d the distance between the X–ray source and the entrance of the capillary and θ_c the critical angle for total reflection.

For our capillaries we calculate, from the above formula, the gain factor listed in Tab.1.

Tab. 1: Theoretical gain factors obtained for different tubes and different capillaries.

∅	**Cu**	**Mo**
100 μm	G=500	G=100
400 μm	G=30	G=10

The high photon flux transmitted does not allow a direct measurement of the beam intensity with the detector positioned in front of the capillary exit. In order to evaluate the true value of the gain factor, we deduced the beam intensity with three independent measurements.

The first one is based on dose measurement performed with a ionisation chamber placed right in front of the capillary outgoing.

In the second case, the intensity transmitted by the capillary was deduced from X ray fluorescence emission. In fact, in the reasonable approximation that the primary X ray beam is nearly monochromatic, the relation between incident radiation intensity, i.e. the intensity transmitted by the capillary, and fluorescence emission from a pure material target is described by a well known formula[8],[9].

In the third case, the intensity outgoing from the X–ray wave–guide was deduced from the detection of the radiation scattered on Plexiglas. We chose an experimental set–up with a scattering angle of 12°, so that the Compton shift was much smaller than the detector resolution, at energies of interest. In this way, with no spectral deformations, calculating for each channel the correction due to cross–sections of scattering processes, we determined the intensity and the spectral distribution of the incident radiation.

Tab. 2: X–rays intensities obtained from scattering, XRF and dose measurements.

Φ=100μm	INTENSITIES FROM SCATTERING MEASUREMENT	INTENSITIES FROM XRF MEASUREMENT	INTENSITIES FROM DOSE MEASUREMENT
Cu	1.0×10^6 cps/mA	9.4×10^5 cps/mA	3.8×10^4 cps/mA
Mo	5.0×10^5 cps/mA	4.5×10^5 cps/mA	2.1×10^4 cps/mA

The intensities obtained from scattering and XRF measurements are in a very good agreement one each other (see Tab.2), while those deduced by dose measurements are more than a factor ten lower. This discrepancy can be justified because the relation between dose and intensity introduces an high error, especially if the radiation field is not strictly monochromatic. Moreover, due to the gain dependence on energy, the spectral distribution from the capillary is deformed with respect to that emerging from the pinhole collimator. So, if we calculate the gain factor using both the intensities deduced by dose measurements, the error is still increased.

For this reason, we think that the values obtained from XRF and scattering measurements are more reliable then those evaluated from dose measurements.

As to the intensities transmitted by the pinhole, they have been estimated using the data available in literature[10],[11] concerning X–ray tubes similar to ours.

In Tab.3, the experimental gain factor for 100 μm capillary are shown as an example.

Tab. 3: Comparison between theoretical and experimental gain factors.

Φ = 100μm	Cu	Mo
Theoretical	G=500	G=100
Experimental	G=50	G=20

It is evident that the experimental values obtained with non–ideal capillaries are affected by absorption of the radiation from the inner walls, as reported also, for instance, by Carpenter[1] and Stern et al.[12], that show a decreasing of more than 70%.

Monocromaticity: Due to the energy dependence of the capillary gain factor[3] ($G \propto E^{-2}$), the monocromaticity of the X–ray source is improved. Consequently, as shown in Fig. 5 for radiation from Mo anode scattered on a low–Z target, the high energy contribution to the spectrum, due to electron bremsstrahlung, is remarkably suppressed and the K_α /K_β ratio increases up to values of about 6.

Diagnostics: In order to verify the beam spot dimension we used a 50 μm copper wire scanning across the beam in 10 μm steps. The differential intensity of the measured XRF line emitted by the wire, plotted as a function of the position, is shown in Fig. 6 for the 100 μm capillary. We obtained a good agreement between experimental and foreseen results, i.e. sharp circular cross–section profile beam with a dimension according to the certified values.

Divergence: Still scanning the beam with the copper wire, we estimated the beam divergence to be (0.17 ± 0.1)°, in close agreement with the attended value (0.18)° corresponding to the critical angle (see Fig. 7). To obtain this value, we evaluated the spot dimension at the distance of 33mm. Then, from the dimension of the beam already determined at the capillary exit, we calculated the divergence angle from geometrical considerations. The error is obtained through the propagation of the uncertainty upon beam diameters (which is of the order of the scanning step of the wire, i.e. 10 μm).

Uniformity: The beam uniformity was checked recording the X–ray image on a fluorescent screen, placed perpendicular to the beam, through a CCD detector. As reported for the 400 μm capillary in Fig. 8, the intensity values along a beam diameter, obtained by image processing, show a gaussian behaviour. In Fig. 9, the recorded image, in grey scale, of the beam spot is shown. The spot is oval due to the angle between the fluorescent screen and the CCD camera. From this measurement we obtain a value for the beam diameter in perfect agreement with the previous evaluation.

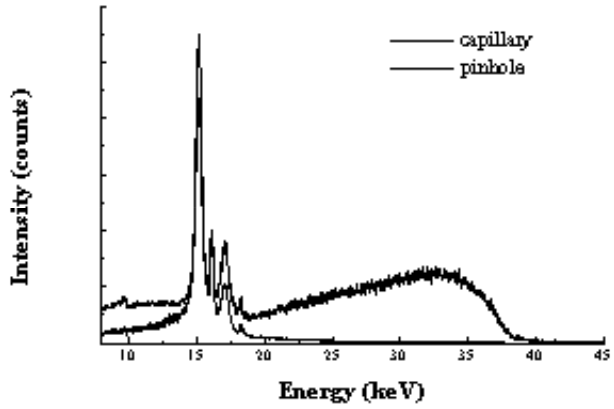

Fig. 5 – Comparison between spectral outgoing distribution, scattered on Plexiglas (θ=135°), with and without the capillary (100μm diameter). The spectra are normalised at K_α Mo Rayleigh peak.

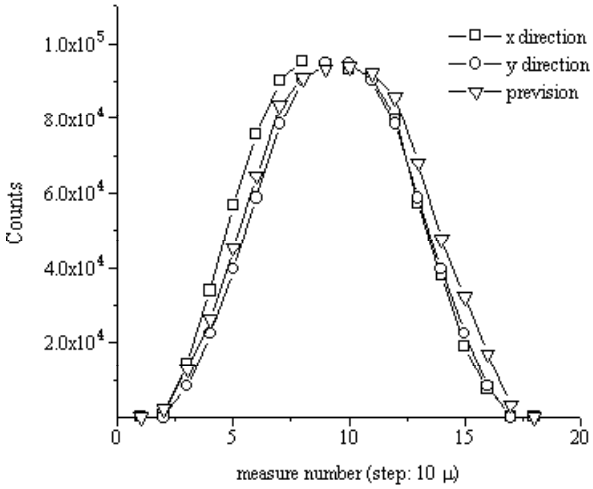

Fig. 6 – Comparison between beam scanning results and calculated values for the scanning of a circular beam with uniform distribution (100μm diameter).

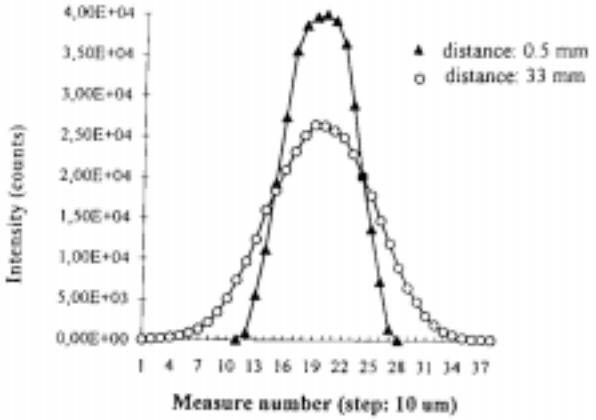

Fig. 7 – Comparison between beam profile scanned at two different distances**.**

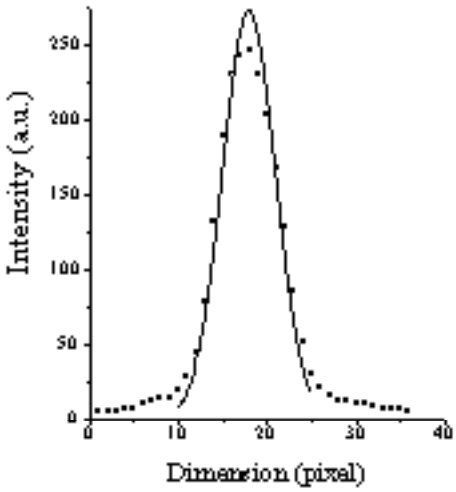

Fig. 8 – Representation of the intensity distribution, along a beam diameter, from the 400 μm capillary.

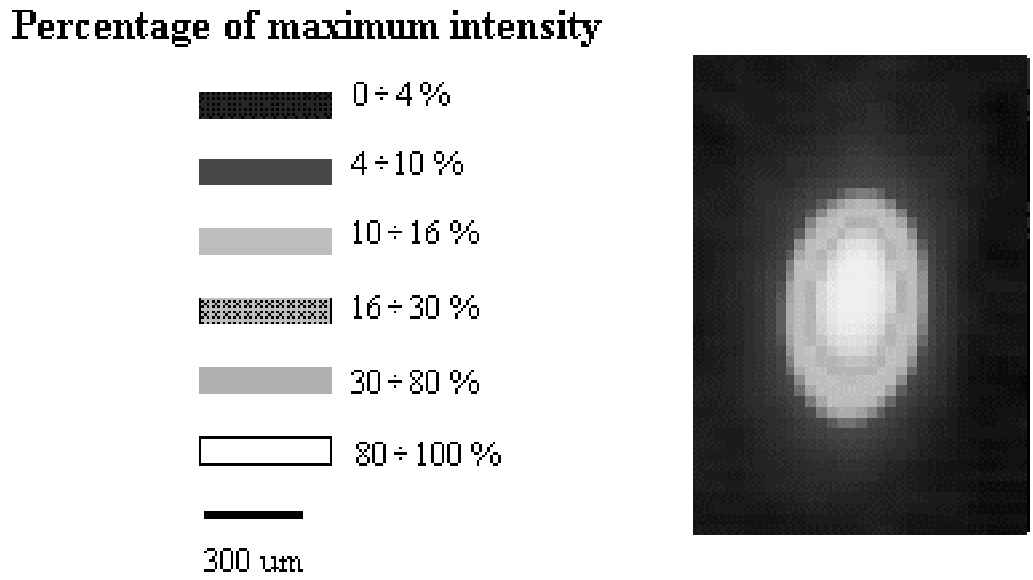

Fig. 9 – Beam image on fluorescent screen as recorded by a CCD camera.

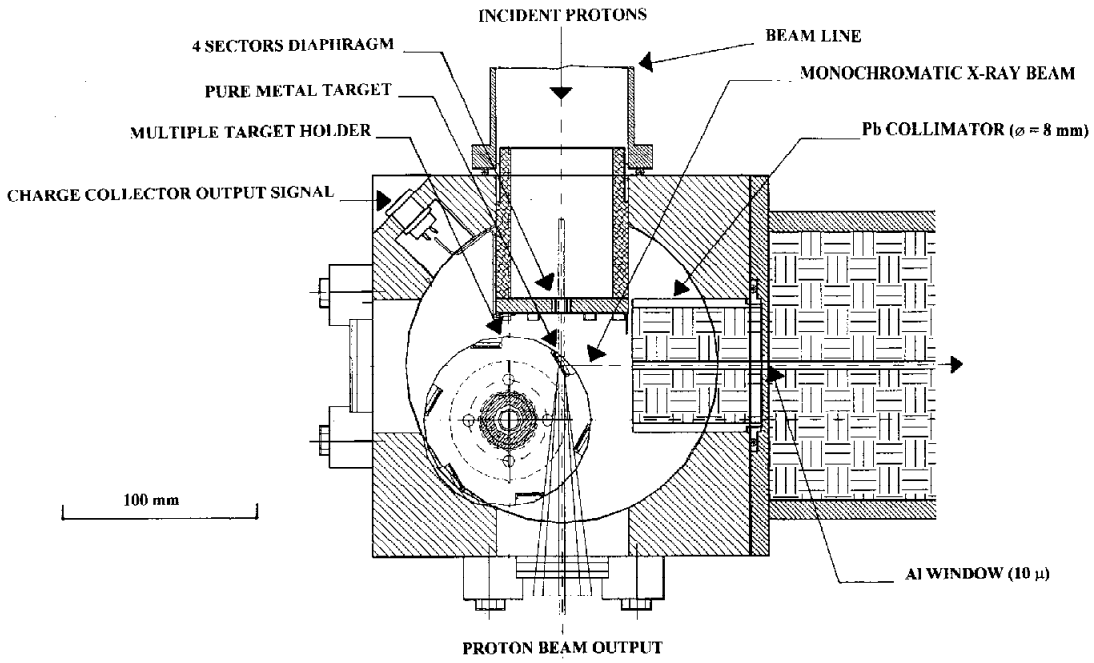

Fig. 10 – Proton irradiation vacuum chamber installed at KN 300 VDG.

4. – CAPILLARY–PIXE INDUCED–XRF MATCHING

A semi–automated, remote–controlled, dual–chamber irradiation system was designed and built for PIXE induced–XRF measurements at KN 3000 VDG accelerator in Florence[7].

As described in the quoted work, the source was characterised in terms of X–ray yield and monocromaticity. The measurements showed a very good spectral purity and high yield values for low–Z targets (see Fig. 6 in Ref. 7).

Using glass microcapillary collimators, we are developing an X–ray source with optical properties well suited for application to XRF analysis. In fact, as shown in Fig.10, replacing the Pb collimator with a glass pipe after moving–back as much as possible the Al window towards the target holder, we plan to obtain an appreciable increase in the beam intensity.

Using a Pb collimator 200 mm long, with inner diameter 400 μm, we estimate a beam intensity on the sample of about 10^2 photons/s for Ge target and about 10^3 photons/s for Cr target, irradiated with 1 cm^2 cross–section 3 MeV, 10 μA proton beam. Using, instead, a capillary of the same length and diameter, taking into account the gain values previously obtained, we could get a beam intensity on the sample about 10 ÷ 70 times greater respectively for Ge and Cr target. This intensity values of the exciting radiation on the sample are still enough for XRF analysis, but a further improvement of a factor 10^2 could be obtained by proper focalisation of the proton beam over smaller spots on the primary targets (∅ ~ 1 mm).

5. – PRELIMINARY APPLICATIONS

To test our spectrometer, the analyses of layered glasses and plaster detachments stratigraphies were performed.

In the former case, we examined the lateral cross–section of some fragments from Roisan Church in Aosta Valley (XVI cent.). The samples consist of layered glasses in which two or three layers, with different compositions, are present. Most of samples have transparent backing and thin layers of coloured glass. The total thickness is about 2 mm and the thickness of each layer varies between 0.2 and 1 mm. Exploiting the reduced size of the beam we scan the lateral cross–section of glass fragments. Qualitative analysis is so obtained for each layer giving information about the characterising elements for the different colours. As to the transparent backing, the different composition give an indication of different origin of the examined glasses. We noted that surface examination of these samples put into evidence some lead content. Since lead was never found from examination of lateral cross–section, we deduced it is due to surface contamination from bindings, as sampling was obtained from the hidden zones under the lead bindings.

In the latter case, the plaster detachments were collected at Serbelloni Palace in Milan. In this case the analysed layer varies in the range between 10 and 100 μm, for a total thickness of about 400 μm. Notwithstanding, with a precise positioning of the sample, scanning the beam across the stratigraphies, it is possible to have some information about the elemental composition of each layer.

ACKNOWLEDGEMENT

We deeply appreciate the help of Dario Giove in the acquisition and treatment of the optical images.

REFERENCES

(1) D. A. Carpenter, *X–Ray Spectrom.* **18**, (1989)
(2) M. C. Nichols, D.R. Boheme, R. W. Ryan, D. Wherry, B. Cross and G. Alden, *Adv. X–Ray Anal.* **30**, (1987)
(3) A. Rinby, P. Engström, S. Larsson and B. Stocklassa, *X–Ray Spectrom.* **18**, (1989)
(4) P. Engström, S. Larsson, A. Rinby and B. Stocklassa, *Nucl. Instr. and Meth.* **B 36**, (1989)
(5) K. Furuta, Y. Nakayama, M. Shoji, H. Nakano and Y. Hosokawa, *Rev. Sci. Instrum.* **62**, (1991)
(6) A. Rinby, *X–Ray Spectrom.* **22**, (1993)
(7) C. Cicardi, C. De Martinis, M. Milazzo and L. Robba, *INFN/TC*–**97/34**, (1997)
(8) C. Bui, L. Confalonieri and M. Milazzo, *Appl. Radiat. Isotop.* **40**, (1989)
(9) M. Milazzo and C. Cicardi, *X–Ray Spectrom.* **26**, (1997)
(10) R.Görgl, P. Wobrauschek, Ch. Streli, H. Aiginger and M. Benedikt, *X–Ray Spectrom.* **24**, (1995)
(11) R. Görgl, P. Wobrauschek, P. Kregsamer and Ch. Streli, *X–Ray Spectrom.* **24**, (1995)
(12) E. A. Stern, Z. Kalman, A. Lewis and K. Lieberman, *Appl. Opt.* **27**, (1988)